PAPER

Photo-assisted water splitting with bipolar membrane induced pH gradients for practical solar fuel devices†

David A. Vermaas,* Mark Sassenburg and Wilson A. Smith*

Different pH requirements for a cathode and an anode result in a non-optimal performance for practical solar fuel systems. We present for the first time a photo-assisted water splitting device using a bipolar membrane, which allows a cathode to operate in an acidic electrolyte while the photoanode is in alkaline conditions. The bipolar membrane dissociates water into H^+ and OH^-, which is consumed for hydrogen evolution at the cathode and oxygen evolution at the anode, respectively. The introduction of such a bipolar membrane for solar fuel systems provides ultimate freedom for combining different (photo)cathodes and -anodes. This paper shows that photo-assisted water splitting at both extreme pH gradients (0–14) as well as mild pH gradients (0–7) yields current densities of 2–2.5 mA cm^{-2} using a $BiVO_4$ photoanode and a bipolar membrane. The membrane potentials are within 30 mV of the theoretical electrochemical potential for low current densities. The pH gradient is maintained for 4 days of continuous operation and electrolyte analysis shows that salt cross-over is minimal. The stable operation of the bipolar membrane in extreme and mild pH gradients, at negligible loss, contributes to a sustainable and practically feasible solar fuel device with existing photoactive electrodes operating at different pH.

Introduction

Direct conversion of solar energy into chemical energy has a huge potential to supply the world with renewable fuel. The incident solar energy of one hour is equivalent to the annual worldwide energy consumption.[1] Several systems have been proposed to utilize solar power for producing a chemical fuel, from which electrochemical water splitting, using either a photovoltaic cell or integrated photoelectrodes, is most intensively studied.[2–8] In these cases, a cathode is used for hydrogen evolution while oxygen is produced at the anode. The activity and stability of each electrode and/or catalyst are strongly dependent on the pH of the electrolyte, due to material corrosion, transport limitations and hydroxyl absorption at the semiconductor surface.[9–12] For example, hydrogen evolution catalysts and ion exchange membranes (*e.g.*, Nafion®) operate well in strongly acidic conditions,[13,14] whereas earth abundant oxygen evolution catalysts are most active and stable in neutral or alkaline conditions.[15–17] Additionally, many photoelectrodes have been investigated at various, narrow pH ranges between 0 and 15.[7] As

there is no consensus about the optimal operating pH for the cathode and anode, with their corresponding catalysts, the options for an integrated solar fuel system are strongly limited.

A bipolar membrane (BPM), traditionally used for the production of acid and base,[18,19] was recently proposed to maintain an acidic cathodic compartment (pH 0) in conjunction with an alkaline anodic compartment (pH 14) for electrolysis.[20,21] Such a configuration could benefit photo-assisted or solar-driven water splitting as well. However, previous research on bipolar membranes only showed low voltage losses at extreme pH-differences (0–14), while it was hypothesized that other pH differences over the membrane would create major voltage losses and unsteady pH differences. This paper demonstrates for the first time effective photo-assisted water splitting using a bipolar membrane induced pH gradient of pH 0 *vs.* 14 as well as pH 0 *vs.* 7, and explores the feasibility for a practical solar fuel application. This research enables the ability to combine a broad spectrum of already developed (photo) electrodes and/or catalysts in their optimal conditions.

Background

A bipolar membrane (BPM) is a polymer membrane composed of a cation exchange layer, selective for cations, and an anion exchange layer, selective for anions. When a current is applied, neither anions or cations can pass both layers, assuming a perfect membrane selectivity. Instead, water is dissociated into H^+ and OH^- at the interface of both ion exchange layers.[22]

Materials for Energy Conversion and Storage (MECS), Department of Chemical Engineering, Faculty of Applied Sciences, Delft University of Technology, Julianalaan 136, 2628 BL Delft, The Netherlands. E-mail: d.a.vermaas@tudelft.nl; w.smith@tudelft.nl
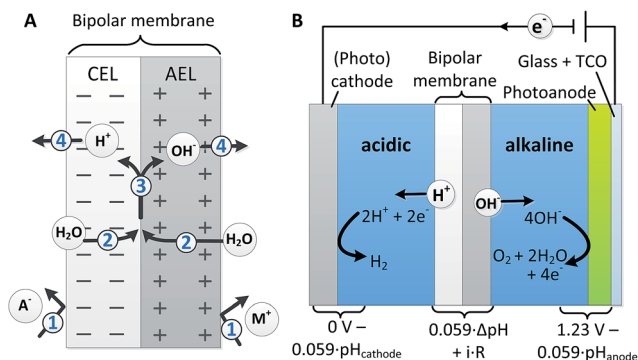
Fig. 1 (A) Working principle of a bipolar membrane. Positive ions (M^+) cannot enter the anion exchange layer (AEL) and negative ions (A^-) cannot enter the cation exchange layer (CEL) (1). This results in water dissociation on the interface of these two layers (3), which is supplied by water diffusion (2) and leads to transport of H^+ and OH^- (4). (B) An example of a bipolar membrane implemented in a solar fuel system, with 1 or possibly 2 photoelectrodes.

The H^+ can pass through the cation exchange layer, while OH^- can pass through the anion exchange layer, as illustrated in Fig. 1A. Assuming 100% faradaic efficiency and high membrane selectivity, the amount of protons and hydroxides produced by water dissociation at the bipolar membrane equals the consumption at the electrodes, which facilitates a constant pH difference over the membrane (Fig. 1B). The driving force required for dissociating water into H^+ and OH^- equals the electrochemical potential difference at the (local) pH in either side of the bipolar membrane layer,[23,24] which results into an electric potential difference $\Delta\Phi_{BPM}$ (in V):

$$\Delta\Phi_{BPM} = \frac{RT}{F}\ln\left(\frac{[H^+]_{cathode}}{[H^+]_{anode}}\right) \approx 0.059\Delta pH \qquad (1)$$

In this equation, R is the universal gas constant (8.31 J mol^{-1} K^{-1}), T is the absolute temperature (K), F is the Faraday constant (96 485 C mol^{-1}), [H$^+$] is the proton concentration at the cathodic and anodic side of the bipolar membrane (M) and ΔpH is the pH difference over the membrane. The chemical potential difference from eqn (1) determines the thermodynamically ideal voltage that is required to drive the water dissociation in the bipolar membrane, and maintain a pH difference between the cathodic and anodic electrolytes. The voltage over the membrane to facilitate the water dissociation causes an equal shift in redox potential for the hydrogen and oxygen evolution reaction, due to the pH difference between anode and cathode (see Fig. 1B). Hence, the total bias over the cell, assuming an ideal membrane, is not increased nor decreased by the water dissociation in the bipolar membrane (see ESI† for further elaboration).

Experimental

Photoanode preparation

BiVO$_4$ photoanodes were prepared in dense thin films of approximately 200 nm, using spray pyrolysis according to the method described in detail by Abdi *et al.*[25] A precursor solution was prepared by dissolving Bi(NO$_3$) (98% pure, Alfa Aesar) in acetic acid (98% pure, Sigma-Aldrich), and added to VO(AcAc)$_2$ (99% pure, Alfa Aesar) dissolved in absolute ethanol (99.8% pure, Sigma-Aldrich). The final concentrations of Bi and V were 4 mM, dissolved in 200 mL solution. This solution was sprayed on FTO (fluorine-doped tin dioxide)-coated glass substrates (TEC-15, Hartford Glass Co.) at 480 °C in 200 cycles. A SnO$_2$ interfacial layer (approximately 80 nm thick, using 0.1 M SnCl$_4$ in ethyl acetate) was sprayed prior to BiVO$_4$ to prevent recombination at the FTO/BiVO$_4$ interface.[26] The FTO/SnO$_2$/BiVO$_4$ samples were annealed for 2 hours in a tube furnace at 450 °C, using continuous flow of air.

For operation at pH 14, the BiVO$_4$ samples were covered with amorphous TiO$_2$ using atomic layer deposition (ALD) as a protective layer for alkaline conditions.[27] TiO$_2$ was deposited in 100 cycles, using tetrakis(dimethylamino)-titanium (TDMAT) and H$_2$O as precursors, deposited at a sample temperature of 100 °C. Each cycle corresponds to approximately 0.1 nm of TiO$_2$, as analysed with ellipsometry (J.A. Woollam Co.) on a Si/TiO$_2$ sample.

Cobalt phosphate (Co-Pi) was electrodeposited on all photoanode samples to catalyse oxygen evolution,[17] using an aqueous solution of 0.1 M potassium phosphate buffer (pH 7.00) and 0.5 mM Co(NO$_3$)$_2$ (99%, Acros Organics). The electrodeposition was performed for 15 minutes at a controlled potential of 1.7 V *vs.* RHE using a potentiostat (PARstat MC, Princeton Applied Research), an AM1.5 light source (100 mW cm^{-2}) and an Ag/AgCl reference electrode (XR300, Radiometer Analytical), corresponding to a CoPi layer thickness of approximately 30 nm.[25]

Water splitting cell

A tailor made polytetrafluoroethylene (PTFE) water splitting cell was used to house the prepared photoanode, bipolar membrane and a planar Pt cathode. The Pt cathode was prepared by sputtering 249 nm of Pt on Ti foil. A commercial bipolar membrane was used (Fumasep FBM, FumaTech), which was conditioned in K$_2$SO$_4$ solution prior to installing in the water splitting cell. The exposed photoanode area was 1.5 cm^2, the cathode area was 4.0 cm^2 and the bipolar membrane area was 19.6 cm^2. The anode was illuminated from the back-side using an AM1.5 solar simulator at 100 mW cm^{-2} (Newport Sol3A Class AAA). The cathodic compartment was filled with 1 M H$_2$SO$_4$ solution (from 95–98% concentrated solution, Sigma-Aldrich), which was separated from the anodic solution by a bipolar membrane as illustrated in Fig. 1B. The anodic compartment was filled with either 1 M phosphate buffer solution with pH 7 (from 99% pure monobasic and 98% pure dibasic potassium phosphate, Sigma-Aldrich) or 1 M KOH solution (from 45% solution, Sigma-Aldrich). A pH meter (ProLine B210, QIS) was installed in both compartments. The anodic compartment was purged with N$_2$ gas at 8 sccm, and the effluent gas was measured using a GC during chronoamperometry. To measure the i–V curve for the bipolar membrane at high current densities (Fig. 4), a Pt electrode was used as an anode and a Luggin capillary was used to

measure the potential near the bipolar membrane. Samples from the anodic and cathodic electrolyte solutions were taken after the experiment and analysed for ionic composition using inductively coupled plasma (ICP-OES 5300 DV).

Electrochemical measurements

Cyclic voltammetry (in dark and illuminated conditions), linear scan voltammetry (chopped illuminated) and chronopotentiometry (illuminated) were performed for the integrated water splitting cell with the bipolar membrane and $BiVO_4$ photoanode. The voltages over each element in the PEC system (cathode, bipolar membrane, photoanode) were monitored using three synchronized potentiostats (PARstat MC, Princeton Applied Research). A detailed description of the voltage measurements is provided in Fig. S1.†

Results

The electrode and membrane potentials are experimentally investigated for a solar assisted water splitting system. For operation at pH 14, samples of $FTO/SnO_2/BiVO_4/TiO_2/CoP_i$ were used as the photoanode. The voltages over each element in the BPM PEC system (cathode, bipolar membrane, photoanode) are shown in Fig. 2 versus the current density of the photoanode,
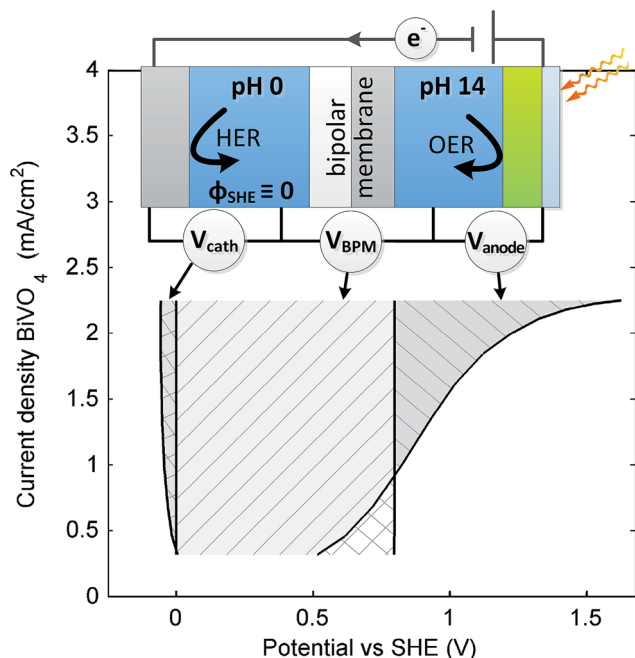

Fig. 2 Potential differences over the cathode (V_{cath}) due to the HER overpotential, over the bipolar membrane (V_{BPM}) and over the anode (V_{anode}), which includes the water reduction potential, the OER overpotential and the photovoltage. The solid lines (from left to right) show the potential of the Pt cathode, SHE reference potential, potential of anode electrolyte (at pH 14) and the $BiVO_4$ photoanode. The cathode operates in pH 0, while the anode operates in pH 14. A standard hydrogen electrode (SHE) scale is used as the pH difference over the membrane disables conversion to RHE. Potentials are obtained from three synchronized potentiostats as illustrated in Fig. S1.† No correction for ohmic losses is applied.

$BiVO_4$. The sum of these voltages represents the total bias applied to the system.

The anode and the bipolar membrane contribute most to the total voltage over the solar fuel system (Fig. 2), while the voltage over the cathode is minor. Although the voltage contribution of the bipolar membrane (V_{BPM}) is significant, it does not imply that a bipolar membrane causes a major loss, as the pH difference established by the bipolar membrane reduces the potential for the oxygen evolution reaction (V_{anode}) $14 \times 0.059 = 0.83$ V. Hence, the voltage over the anode is even negative for low current densities (<1 mA cm^{-2}), causing an intersection of the BPM and anode potentials in Fig. 2, which implies the magnitude of the photovoltage is larger than the oxygen evolution potential plus overpotential in this pH.

At pH 14, a current density of approximately 2 mA cm^{-2} is obtained at the water oxidation potential (1.23 V vs. SHE), corresponding to a total bias of approximately 1.3 V in this bipolar membrane device. Significantly larger potential differences over the photoanode are required to obtain higher current densities. Because the redox potential for oxygen evolution and the photovoltage of $BiVO_4$ are independent of the current density, this trend is due to the overpotential for the oxygen evolution reaction. This limited current density at higher potentials is also observed in cyclic voltammetry of the $BiVO_4/TiO_2/CoPi$ samples (Fig. S2†). The exact mechanisms of this behavior is beyond the scope of this paper, but may be related with the TiO_2 layer, as $BiVO_4/CoPi$ demonstrates a higher current density than $BiVO_4/TiO_2/CoPi$ at pH 7 (see ESI†).

To fully exploit the ability of having different pH's at either side of the bipolar membrane, photo-assisted water splitting was also performed at pH 0 (cathode) vs. pH 7 (anode), which allows the ability to use $BiVO_4/CoPi$ without a TiO_2 layer. At this pH difference, current densities of more than 2.5 mA cm^{-2} are obtained at a bias of approximately 1.3 V, as shown in Fig. 3. Faradaic efficiencies of nearly 100% are obtained for $BiVO_4$ (for O_2 evolution) and Pt (for H_2 evolution) in previous research.[28] Our data, using gas chromatography (Fig. S5†), confirms that oxygen was evolved at high faradaic efficiency at the $BiVO_4/CoPi$ photoanode. Hence, when envisioning a solar fuel device with a double junction a-Si photovoltaic cell behind the photoanode, as demonstrated by Abdi et al.,[29] the obtained current density would correspond to a solar-to-hydrogen (STH) efficiency of 3.0% (see Fig. S4†). This yield can be improved using a higher performing photoelectrode, such as doped $BiVO_4$ (ref. 29) or Si-based photoelectrodes.[30–32]

Compared to the total bias over a $BiVO_4$–Pt system operating in a single pH without using a membrane, the bias over the BPM system is similar or even smaller (see Fig. S4†). In other words, the use of a bipolar membrane in solar fuel systems, thereby enabling a pH difference between cathode and anode, features no significant thermodynamic loss.

In more detail, the voltages over the bipolar membrane are even slightly smaller than the theoretical voltages required for maintaining this pH difference, in particular for the case with pH 0 vs. pH 7 (Fig. 3), where 0.41 V is theoretically required for maintaining a difference of 7 pH units. The lower actual membrane voltage is due to imperfections in selectivity of the
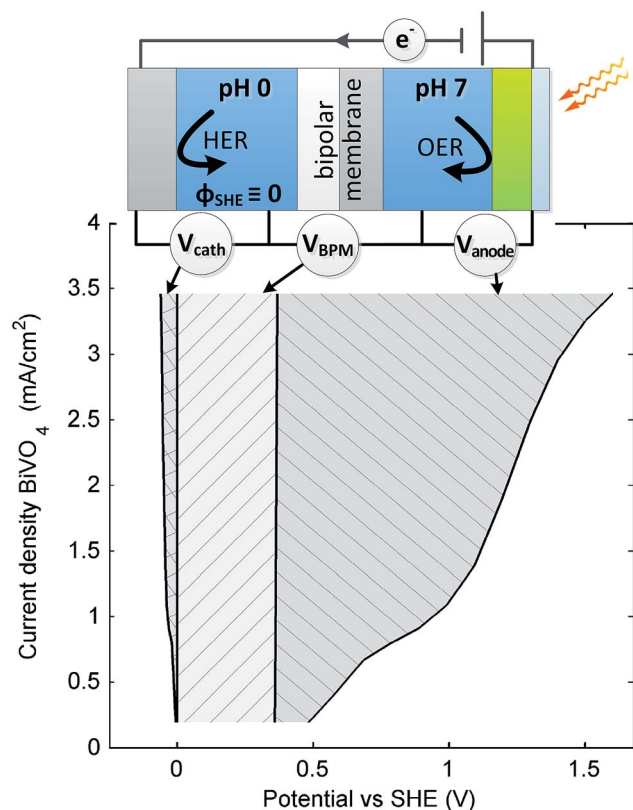
19558 | J. Mater. Chem. A, 2015, 3, 19556–19562

This journal is © The Royal Society of Chemistry 2015

Fig. 3 Potential differences over the cathode (V_{cath}), over the bipolar membrane (V_{BPM}) and over the anode (V_{anode}), obtained in the same configuration as for Fig. 2, except that the anode operates in pH 7 in this case. No correction for ohmic losses is applied.

Fig. 4 Voltage over the bipolar membrane using a pH difference of 0–7 and 0–14 over the membrane as a function of the current density. The potentials were averaged over at least 300 s of constant current. As the bipolar membrane (BPM) area was larger than the BiVO$_4$ area, the corresponding current density for BiVO$_4$ is plotted as a secondary x-axis. No correction for ohmic losses is applied.

membrane. As the membrane layers are in reality not perfectly selective for anions and cations, other ions than H^+ or OH^- can pass the BPM as well, although at small rates. Consequently, K^+ and SO_4^{2-} can be transported through the BPM to some extent. The transport of these ionic species is not limited to the theoretical water dissociation voltage,[22,33] which explains the slightly lower than theoretical membrane voltage shown in Fig. 2 and 3.

Whereas efficient use of a bipolar membrane for extreme pH gradients is acknowledged in literature,[24,33] the use of BPMs for milder pH gradient was found to have relatively large membrane voltages. According to eqn (1), the thermodynamically ideal membrane voltage over the bipolar membrane should be 0.83 V for a difference of 14 pH units (*i.e.*, 14 × 0.059), while 7 pH units should yield a membrane voltage of 0.41 V (*i.e.*, 7 × 0.059). Previous research predicted that a membrane voltage of >0.8 V would be necessary to drive water dissociation for mild pH gradients as well,[21] based on experiments at high current densities, typical for existing bipolar membrane applications.[23] However, solar fuel devices need to operate at much lower current densities (order of 10 mA cm^{-2}) compared to previous applications of bipolar membranes (typically 100 mA cm^{-2}).[23]

The bipolar membrane voltages are plotted as a function of the current density in Fig. 4. Our results confirm the predicted large membrane voltages over the BPM using a pH gradient of 0–7 for high current densities (Fig. 4). At low current density, the membrane voltage is actually close to the thermodynamically
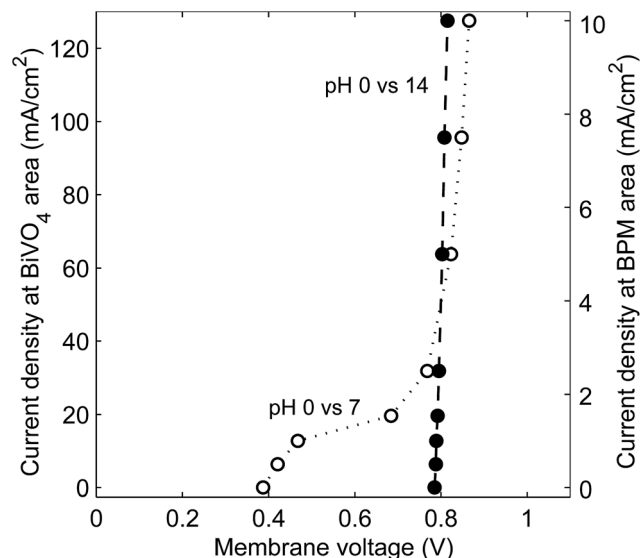
ideal case for a pH gradient of 0 and 7 (0.41 V). Although the current density scaled on the membrane area is rather low (<2 mA cm^{-2}) for this effect, it provides evidence for this phenomenon and raises the question whether and how this region can be extended to higher current densities.

The transport at these particular conditions (low current and mild pH gradients) are not well explored yet, while crucial for the solar fuel application. Previous research indicated that charge transport at low current densities was ascribed to leakage of co-ions through the BPM,[20,33] which would sacrifice the pH difference. To experimentally investigate the dominant charge transport though the BPM at low current densities, the membrane voltage, pH and ion concentrations are monitored for 4 days of continuous operation using an inert (Pt) electrode at either side, shown in Fig. 5. The voltages and the pH differences over the bipolar membrane slowly decrease, but still a significant pH difference over the bipolar membrane remains after four days. The largest difference in pH is observed for pH 7, because the pK_a of phosphate is slightly higher than 7, which makes this buffer most sensitive to acidification. If the ion transport would be dominated by other ions than H^+ and OH^-, the pH difference would have been completely disappeared at charge transport of 1 mole equivalent. As the pH difference is maintained for the greater part after charge transport of 1 mole equivalent, the transport through the bipolar membrane must by dominated by H^+ and OH^-.

In addition, samples from the cathodic and anodic electrolyte after four days reveal that only a small fraction of the potassium, and no significant sulphates or phosphates have been transported through the membrane (Table 1). Only a small fraction of the potassium, and no significant sulphates or phosphates have been transported through the membrane. The
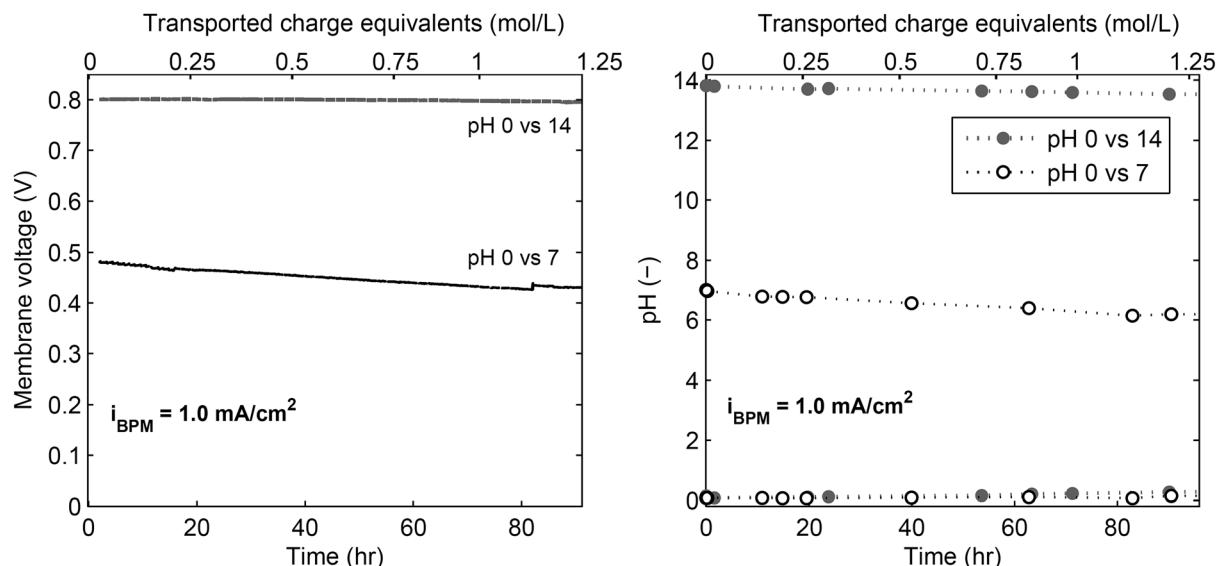
Fig. 5 Membrane voltage (left) and pH (right) as a function of time, at a constant current density of 1 mA cm^{-2} of BPM area (which corresponds to 12.8 mA cm^{-2} anode area in this case). Inert (Pt) electrodes were used as anode and cathode in this case.

high rejection rate for sulphates and phosphates is due to the larger hydrated radius and larger charge of these ions, which increases the rejection of these co-ions in ion exchange membranes.[34] The data in Table 1 indicates that water dissociation dominates over salt cross-over, and hence bipolar membranes can be applied to maintain a pH difference acceptably in a practical water splitting device at low current densities as well.

Having established that the water dissociation in the bipolar membrane causes the dominant transport mechanism, even at low current densities, the obtained membrane voltage–current curve for the pH 0–7 case in Fig. 4 requires a different explanation than co-ion transport. The large membrane voltages at high current densities can be explained from ion transport limitations near the BPM–water interfaces.[35] A stagnant diffusive boundary layer will be created at the membrane–water interface when higher current densities are applied, which increases the pH difference between the two membrane–water interfaces (i.e., concentration polarization),[36] as illustrated in

Scheme 1. In this schematic representation, the internal pH in the anion exchange layer (AEL) is assumed to be close to 14.[21] When no significant current is applied, a Donnan potential exists at the AEL–water interface, due to the sudden change in OH$^-$ concentration and the selectivity for anions only. This Donnan potential adds to the voltage for water dissociation at the AEL–CEL interface, which yields a total membrane voltage of approximately 0.4 V (i.e., 7 pH units in eqn. (1)) at low current densities (Scheme 1A). At higher current densities, a diffusive boundary layer builds up near the membrane–water interface, which causes a higher pH in the electrolyte near the membrane surface. Hence, the concentration polarization reduces the Donnan potential at the membrane surface and leads to a higher membrane voltage, as observed in Fig. 4.

Such a mechanism predicts that a low membrane voltage can be maintained for higher current densities as well when the mass transport in the electrolyte is improved. This implies that a bipolar membrane system, offering a different anodic and cathodic regime in term of pH and possibly electrolyte

Table 1 pH and concentrations of cathodic and anodic solutions in the case of a pH 0−7 difference over the bipolar membrane, before and after 4 days of operation at 1 mA cm^{-2}. Concentrations are derived from ICP analysis

Solution	pH	[K$^+$] (in M)	Sulphates (M)	Phosphates (M)
Cathodic solution				
1 M H$_2$SO$_4$ (as should be)	0.00^a	0.00	1.00	0.00
1 M H$_2$SO$_4$ (as measured)	0.08	<0.02	1.02 ± 0.07	<0.02
After 4 days	0.14	0.29 ± 0.04	0.99 ± 0.07	<0.02
Anodic solution				
1 M phosphate buffer (as should be)	7.00	1.39	0.00	1.00
1 M phosphate buffer (as measured)	7.01	1.48 ± 0.09	<0.02	1.00 ± 0.07
After 4 days	6.15	1.30 ± 0.08	<0.02	1.03 ± 0.07

^{a} Neglecting the activity coefficient of H$_2$SO$_4$.
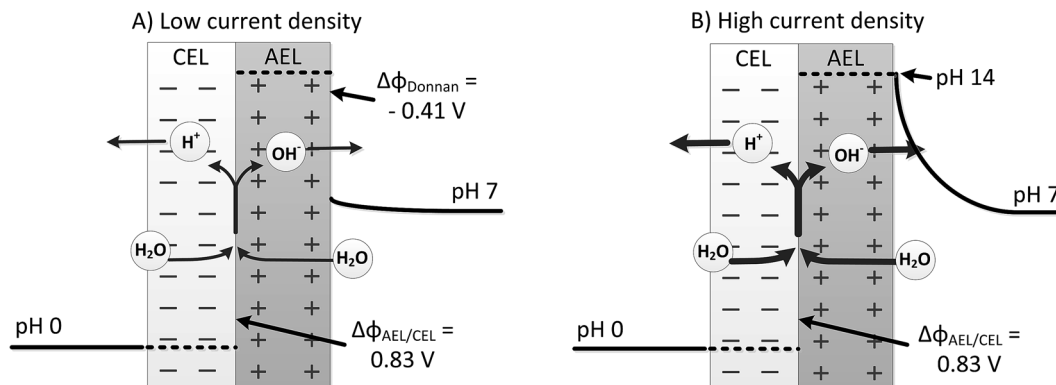
Scheme 1 Bipolar membrane with internal (dotted line) and external (solid line) pH profiles, as hypothesized for low current density (A) and higher current density (B). The internal pH is assumed to be 0 in the cation exchange layer (CEL) and 14 in the anion exchange layer (AEL).

composition, provides ultimate freedom to allow operation of (photo)electrodes at maximum efficiency and stability.

Conclusions

For the first time, photo-assisted water splitting is performed with an acidic cathodic compartment and a neutral or alkaline anodic compartment. Such pH gradients are maintained using a bipolar membrane, where water is dissociated into H^+ and OH^- and these ions are transported to the cathode and anode, respectively. Hence, water splitting is demonstrated using Pt as a cathode in pH 0 and $BiVO_4$ as a photoanode in pH 7 and pH 14. The measured voltage over the bipolar membrane is close to the thermodynamic potential difference to maintain the pH difference between cathode and anode and the bias over the total system is similar or even slightly smaller than using a PEC system in a single pH compartment. A photocurrent of 2.5 and 2 mA cm^{-2} is obtained at 1.3 V bias, for both pH gradients of 0–7 and 0–14, respectively. A minor fraction of other ions than H^+ and OH^- is transported through the membrane due to imperfect selectivity of the membrane layers. This results in a membrane voltage that is slightly lower than the thermodynamically required voltage, at the expense of a slowly decreasing pH difference over the membrane. While previous work predicted that a bipolar membrane can only be used efficiently at extreme pH gradients, our data shows that a pH gradient of 0–7 works stable and without significant voltage loss when operated at current densities commensurate with those proposed for solar fuel generators. Transport of H^+ and OH^- remains the main transport mechanism in the bipolar membrane, even at low current density or using neutral pH in the anodic electrolyte. Therefore, the use of a bipolar membrane expands the possibilities for practical solar fuel designs.

Acknowledgements

References

1 *International Energy Agency (IEA)*, ed. C. Philibert, 2014, p. 55.
2 J. Jin, K. Walczak, M. R. Singh, C. Karp, N. S. Lewis and C. Xiang, *Energy Environ. Sci.*, 2014, **7**, 3371–3380.
3 O. Khaselev and J. A. Turner, *Science*, 1998, **280**, 425–427.
4 C. Rodriguez, M. A. Modestino, C. Moser and D. Psaltis, *Energy Environ. Sci.*, 2014, **7**, 3828–3835.
5 P. Bornoz, F. F. Abdi, S. D. Tilley, B. Dam, R. van de Krol, M. Graetzel and K. Sivula, *J. Phys. Chem. C*, 2014, **118**, 16959–16966.
6 S. Haussener, S. Hu, C. Xiang, A. Z. Weber and N. S. Lewis, *Energy Environ. Sci.*, 2013, **6**, 3605–3618.
7 J. W. Ager, M. Shaner, K. Walczak, I. D. Sharp and S. Ardo, *Energy Environ. Sci.*, 2015, DOI: 10.1039/c1035ee00457h.
8 J. R. McKone, N. S. Lewis and H. B. Gray, *Chem. Mater.*, 2014, **26**, 407–414.
9 M. G. Walter, E. L. Warren, J. R. McKone, S. W. Boettcher, Q. Mi, E. A. Santori and N. S. Lewis, *Chem. Rev.*, 2010, **110**, 6446–6473.
10 T. W. Hamann, F. Gstrein, B. S. Brunschwig and N. S. Lewis, *Chem. Phys.*, 2006, **326**, 15–23.
11 S. Y. Reece, J. A. Hamel, K. Sung, T. D. Jarvi, A. J. Esswein, J. J. H. Pijpers and D. G. Nocera, *Science*, 2011, **334**, 645–648.
12 H. Gerischer, *Electrochim. Acta*, 1989, **34**, 1005–1009.
13 P. C. K. Vesborg, B. Seger and I. Chorkendorff, *J. Phys. Chem. Lett.*, 2015, **6**, 951–957.
14 E. Navarro-Flores, Z. Chong and S. Omanovic, *J. Mol. Catal. A: Chem.*, 2005, **226**, 179–197.
15 C. C. L. McCrory, S. Jung, J. C. Peters and T. F. Jaramillo, *J. Am. Chem. Soc.*, 2013, **135**, 16977–16987.
16 C. C. L. McCrory, S. Jung, I. M. Ferrer, S. M. Chatman, J. C. Peters and T. F. Jaramillo, *J. Am. Chem. Soc.*, 2015, **137**, 4347–4357.
17 M. W. Kanan and D. G. Nocera, *Science*, 2008, **321**, 1072–1075.

18 L. Bazinet, F. Lamarche and D. Ippersiel, *Trends Food Sci. Technol.*, 1998, **9**, 107–113.

19 X. Tongwen, *Resour., Conserv. Recycl.*, 2002, **37**, 1–22.

20 M. B. McDonald, S. Ardo, N. S. Lewis and M. S. Freund, *ChemSusChem*, 2014, **7**, 3021–3027.

21 N. M. Vargas-Barbosa, G. M. Geise, M. A. Hickner and T. E. Mallouk, *ChemSusChem*, 2014, **7**, 3017–3020.

22 H. Strathmann, J. J. Krol, H. J. Rapp and G. Eigenberger, *J. Membr. Sci.*, 1997, **125**, 123–142.

23 A. Alcaraz, P. Ramírez, S. Mafé, H. Holdik and B. Bauer, *Polymer*, 2000, **41**, 6627–6634.

24 J. J. Krol, PhD thesis, Universiteit Twente, 1997, p. 164.

25 F. F. Abdi and R. van de Krol, *J. Phys. Chem. C*, 2012, **116**, 9398–9404.

26 Y. Liang, T. Tsubota, L. P. A. Mooij and R. van de Krol, *J. Phys. Chem. C*, 2011, **115**, 17594–17598.

27 S. Hu, M. R. Shaner, J. A. Beardslee, M. Lichterman, B. S. Brunschwig and N. S. Lewis, *Science*, 2014, **344**, 1005–1009.

28 B. J. Trzesniewski and W. A. Smith, *J. Mater. Chem. A*, 2015, DOI: 10.1039/c1035ta04716a.

29 F. F. Abdi, L. Han, A. H. M. Smets, M. Zeman, B. Dam and R. van de Krol, *Nat. Commun.*, 2013, **4**, 2195–2201.

30 I. A. Digdaya, L. Han, T. W. Buijs, M. Zeman, B. Dam, A. H. Smets and W. A. Smith, *Energy Environ. Sci.*, 2015, **8**, 1585–1593.

31 M. J. Kenney, M. Gong, Y. Li, J. Z. Wu, J. Feng, M. Lanza and H. Dai, *Science*, 2013, **342**, 836–840.

32 C. G. Morales-Guio, K. Thorwarth, B. Niesen, L. Liardet, J. Patscheider, C. Ballif and X. Hu, *J. Am. Chem. Soc.*, 2015, **137**, 7035–7038.

33 F. G. Wilhelm, I. Pünt, N. F. A. van der Vegt, M. Wessling and H. Strathmann, *J. Membr. Sci.*, 2001, **182**, 13–28.

34 D. A. Vermaas, J. Veerman, M. Saakes and K. Nijmeijer, *Energy Environ. Sci.*, 2014, **7**, 1434–1445.

35 F. G. Wilhelm, N. F. A. van der Vegt, H. Strathmann and M. Wessling, *J. Membr. Sci.*, 2002, **199**, 177–190.

36 A. A. Sonin and G. Grossman, *J. Phys. Chem.*, 1972, **76**, 3996–4006.